SUPPLEMENTAL INFORMATION TITLES AND LEGENDS

Supplemental figure legends

Fig. S1. Necrotic lung granulomas in Mtb-infected mice subsequently challenged with LCMV CL13. C57BL/6 mice were infected with Mtb. Some mice from each group were subsequently infected 14 days later with LCMV CL13. At 31 days post Mtb infection, the mice were sacrificed. **a,** Gross pathology of the lung. **b,** H&E staining or **c,** acid-fast staining of the lung in each group. (10x, Scale bars, 2 mm., 400x, Scale bars, 50μm). **d,** The data represent the percentage of the superior lobe of the right lung showing inflammation and are shown as box-and-whisker plots showing the minimum and maximum values. **e,** Bacterial load in the organs of each group. **f,** Survival was monitored at the indicated time points after CL13 infection. **d, e,** The data were analyzed by two-tailed unpaired Student's *t* test, and **f,** survival graphs were analyzed using the Mantel-Cox log-rank test. Plots show the mean ± SEM. **a-f,** The data are representative of at least two independent experiments (n=4-5 mice/group). **P*<0.05; ***P*<0.01; ****P*<0.001; *****P*<0.0001.

Fig. S2. Flow cytometry gating strategy for elucidation of myeloid cell populations in the lung and analysis of pulmonary immune cells and cytokines. a, Lungs were harvested, and cells were stained for cell surface expression of CD11b, Ly6G, and Ly6C. To define the myeloid cell population in the lung, total lung cells were pregated on single cells, FSC-A^{hi} SSC-A^{hi} (leukocytes), and live cells and excluded by $Thy1.2^{+}$, $NK1.1^{+}$, and $CD19^{+}$ signals. **b,** C57BL/6 mice were infected with Mtb. Some mice from each group were subsequently infected 14 days later with LCMV Arm. At days 3-17 post LCMV Arm infection, immune cells in the lung were isolated and analyzed by flow cytometry. Each immune cell population is summarized in the plot. **c,** At 17 days post LCMV Arm infection, the IL-10 level in the lung was measured by ELISA. **d,** At days 3-17 post LCMV Arm infection, the IL-1α and IL-1β levels in lung homogenates were analyzed by ELISA. **b, d,** The data were analyzed by two-way ANOVA with *post hoc* Tukey's test or **c,** two-tailed unpaired Student's *t* test. Plots show the mean ± SEM. **b,** The data are representative of at least two experiments (n=4-5 mice/group) or **c, d,** a single experiment (n=3-4 mice/group). n.s., not significant. **P*<0.05; ***P*<0.01; ****P*<0.001; *****P*<0.0001.

Fig. S3. Prevention of exacerbated pulmonary immunopathology by BCG vaccination or the preexistence of Mtb-specific IFN-γ-producing cells *in vivo*. a, C57BL/6 mice were vaccinated 3 months before challenge with Mtb. At 3 months after mice were infected with Mtb, some mice from each group were subsequently infected with LCMV Arm 14 days later. **b,** Gross pathology of the lung and **c,** H&E staining of the lung in each group. Scale bars, 2 mm. **d,** Bacterial loads in the lung. **e,** The frequency of $CD11b^+Ly6G^+$ cells at 7 days post LCMV Arm infection is summarized in the plot. **f-g,** Frequencies of IFN-γ- and TNF-α-producing $CD4^+$ T cells were analyzed by flow cytometry. **h,** C57BL/6 mice were infected with Mtb. Some mice from each group were subsequently infected with Arm at the indicated time points after Mtb infection. **i,** At 14 days or 21 days post Mtb infection (before LCMV Arm infection), isolated lung lymphocytes were restimulated *ex vivo* with an ESAT6 pool containing all peptides. The frequencies of IFN-γ- and TNF-α-producing $CD4^+$ T cells were analyzed by flow cytometry. **j-l,** At 31 days post Mtb infection, the mice were sacrificed. **j,** Gross pathology or **k,** H&E staining of the lungs in each group. Scale bars, 2 mm. **l,** Bacterial load of the lung in each group. The data were analyzed by **d, e, g, and l,** one-way ANOVA with *post hoc* Tukey's test or **i,** two-tailed unpaired Student's *t* test. Plots show the mean ± SEM. **a-g,** The data are representative of a single experiment (n=4-5 mice/group). n.s., not significant. **P*<0.05; ***P*<0.01; ****P*<0.001; *****P*<0.0001.

Fig. S4. Effect of blockade or depletion of immunological factors on pulmonary pathology and analysis of the characteristics of CD11b$^+$Ly6G$^+$ populations. a-h, C57BL/6 mice were infected with Mtb. Some mice from each group were subsequently infected 14 days later with LCMV Arm. At the indicated time points, a monoclonal antibody was administered i.p. into coinfected mice. The mice were sacrificed at 31 days post Mtb infection. **b, f,** Gross pathology or **c, g,** H&E staining of the lung in each group. **d, h,** Bacterial loads in the lung of each group. **i,** Representative cell isolation gating strategy for the CD11b$^+$Ly6G$^+$ cell population. **j,** At 4 weeks post infection, equal numbers of isolated CD11b$^+$Ly6G$^+$ cells from Mtb-infected and coinfected mice were lysed with 0.05% Triton-X 100, and the lysates were plated onto 7H10 agar to enumerate the bacteria. **k, l,** Naïve splenic T cells were stimulated with anti-CD3 and CD28 monoclonal antibodies in the absence or presence of CD11b$^+$Ly6G$^+$ cells isolated from the lungs of Mtb-infected or coinfected mice at 21 days post Mtb infection. **k,** Flow cytometry data showing the proliferation of CD4$^+$ or CD8$^+$ T cells assessed by a Cell Trace Violet (CTV) dilution assay. **l,** CTV$^+$CD4$^+$ T cells and CD8$^+$ T cells are summarized in the graph. The numbers in the plots indicate the percentage of CTV$^+$CD4$^+$ T cells and CD8$^+$ T cells. The data were analyzed by **d, h, l,** one-way ANOVA with *post hoc* Tukey's test or **j,** two-tailed unpaired Student's *t* test. Plots show the mean ± SEM. **a-h,** The data are representative of at least two independent experiments (n=3-5 mice/group) or **i-l,** representative of a single experiment (n=2 wells/group). n.s., not significant. **P*<0.05; ***P*<0.01; ****P*<0.001; *****P*<0.0001.

Fig. S5. Viral titers and LCMV-specific T cell responses during infection and the effect of type I IFN blockade on the expression level of MHCII in DCs. a, Serum was collected on the indicated days from each group of mice, and the virus titer was determined. The dashed line indicates the limit of virus detection. Undetectable samples are represented as half of the detection limit. **b-e,** Isolated lung lymphocytes were restimulated *ex vivo* with the GP33 and GP276 peptides for $CD8^+$ T cell responses or the GP66 peptide for $CD4^+$ T cell responses. **b, d,** Frequencies of IFN-γ- and TNF-α-producing T cells were analyzed by flow cytometry, and **c,** the frequencies of $CD4^+$ T cells and **e,** $CD8^+$ T cells producing both IFN-γ and TNF-α in the lung are summarized in the plot. **f-i,** DCs were isolated from **f,** LNs at 7 days post LCMV Arm infection or **h,** lungs at the indicated days post LCMV Arm infection, and MHCII expression on DCs was analyzed by flow cytometry. Numbers in the plots indicate the mean fluorescence intensity (MFI) of MHCII on DCs. The MFI values of MHCII in **g,** LNs or **i,** lungs are also summarized in graph. The data were analyzed by **a-g,** one-way ANOVA with *post hoc* Tukey's test or **i,** two-way ANOVA with *post hoc* Tukey's test. Plots show the mean ± SEM. The data are representative of at least two independent experiments (n=4-5 mice/group). *P<0.05; **P<0.01; ***P<0.001; ****P<0.0001.

Fig. S6. Exacerbated pulmonary pathology of the lungs of mice injected with poly I:C. a, C57BL/6 mice were infected with Mtb. Some mice from each group were subsequently infected 14 days later with LCMV Arm or injected with poly I:C. The mice were sacrificed at 31 days post Mtb infection. **b,** Gross pathology or **c,** H&E staining of the lungs in each group. **d,** Bacterial loads in the lungs of each group. **e-h,** Isolated lung lymphocytes were restimulated *ex vivo* with the **e-f,** ESAT6 peptide pool or **g-h,** Mtb32 peptide pool. The frequencies of IFN-γ- and TNF-α-producing T cells were analyzed by flow cytometry. **i,** C57BL/6 mice were infected with LCMV Arm or injected with poly I:C. Serum was collected at the indicated time points, and IFN-α levels were analyzed by ELISA. The data were analyzed by **i,** two-tailed unpaired Student's *t* test and **d, f, h,** one-way ANOVA with *post hoc* Tukey's test. Plots show the mean ± SEM. **a-h,** The data are representative of a single experiment (n=4-9 mice/group). n.s., not significant. **P*<0.05; ***P*<0.01; ****P*<0.001; *****P*<0.0001.

Fig. S7. Alteration of T cell signatures by coinfection. a, UMAP plots of mean gene expression for Th1 and activation signatures. **b,** UMAP plots of mean gene expression for the effector $CD8^+$ T cell signature. **c,** Violin plots showing the expression of the indicated marker genes from the indicated T cell clusters. **d,** The number of unique or expanded clonotype cells in the effector $CD8^+$ T cell clusters is summarized in the bar graph. N/A indicates “not available” populations, which means that the gray bar represents the nonunique or expanded clonotypes. The $CD45^+$ immune cells were pooled from mice (n=3) in each group. The data were analyzed by Wilcoxon rank sum test. n.s., not significant. *P<0.05; **P<0.01; ***P<0.001; ****P<0.0001.

Fig. S8. Graphical abstract of our experiments. (Left) When Mtb-speicific Th1 responses were preexisted in some cases like BCG immunization, Mtb-specific Th1 cells were properly activated and proliferated in draing lymph node and then migrated to pulmonary leisons for protect host from Mtb. **(Right)** On the other hand, when mice were exposed to high levels of type I IFN production such as LCMV infection *in vivo*, migration of Mtb-specific Th1 cells were hindered by down-regulation of CXCL9/10 expression through type I IFN dependent manner. The reduced Mtb-specific Th1 cells in pulmonary leisons triggered Mtb dissemination and pathology exacerbation due to low levels of IFN-γ of Mtb-specific T cells.

Supplementary Figure 1

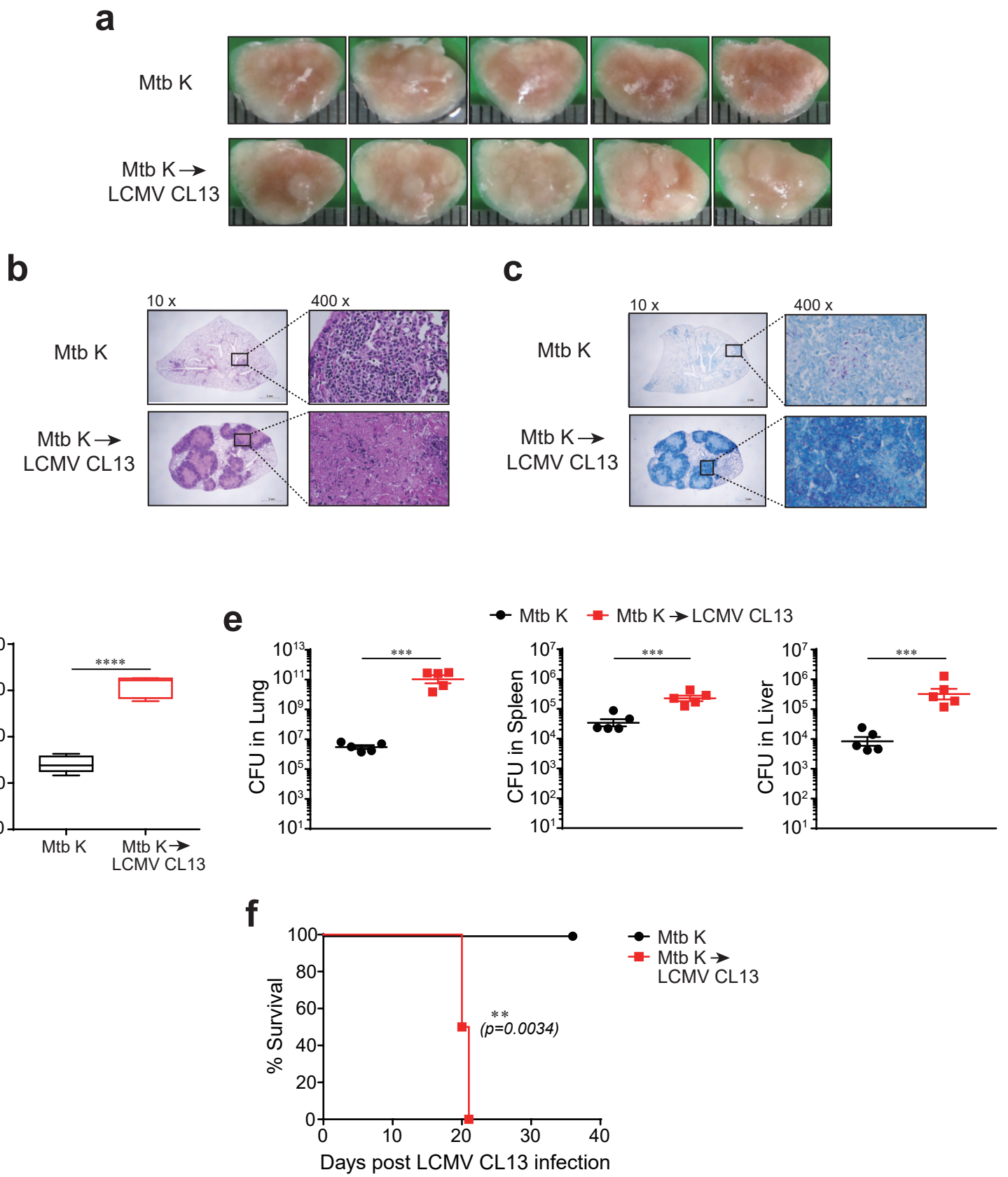

Supplementary Figure 2

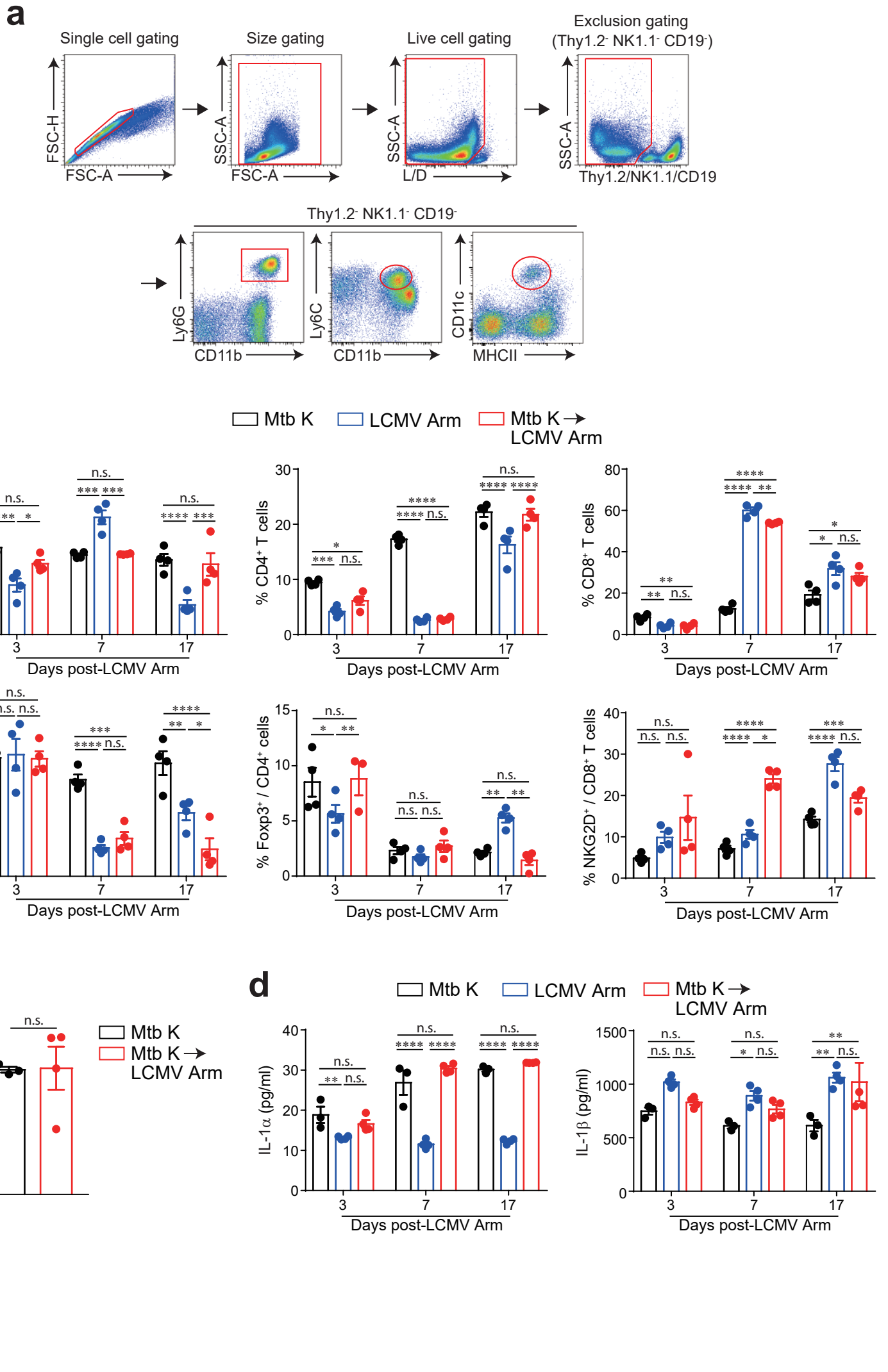

Supplementary Figure 3

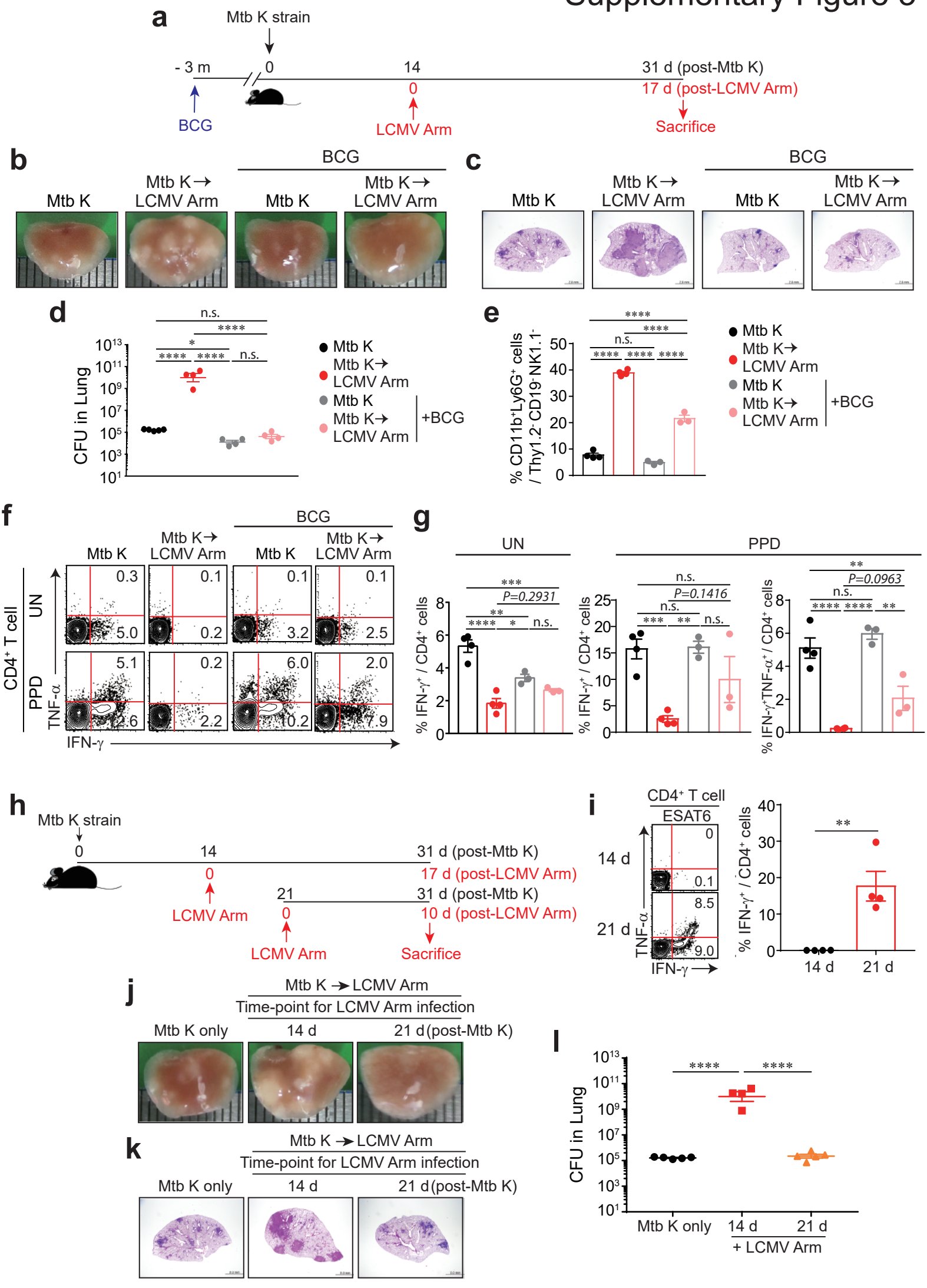

Supplementary Figure 4

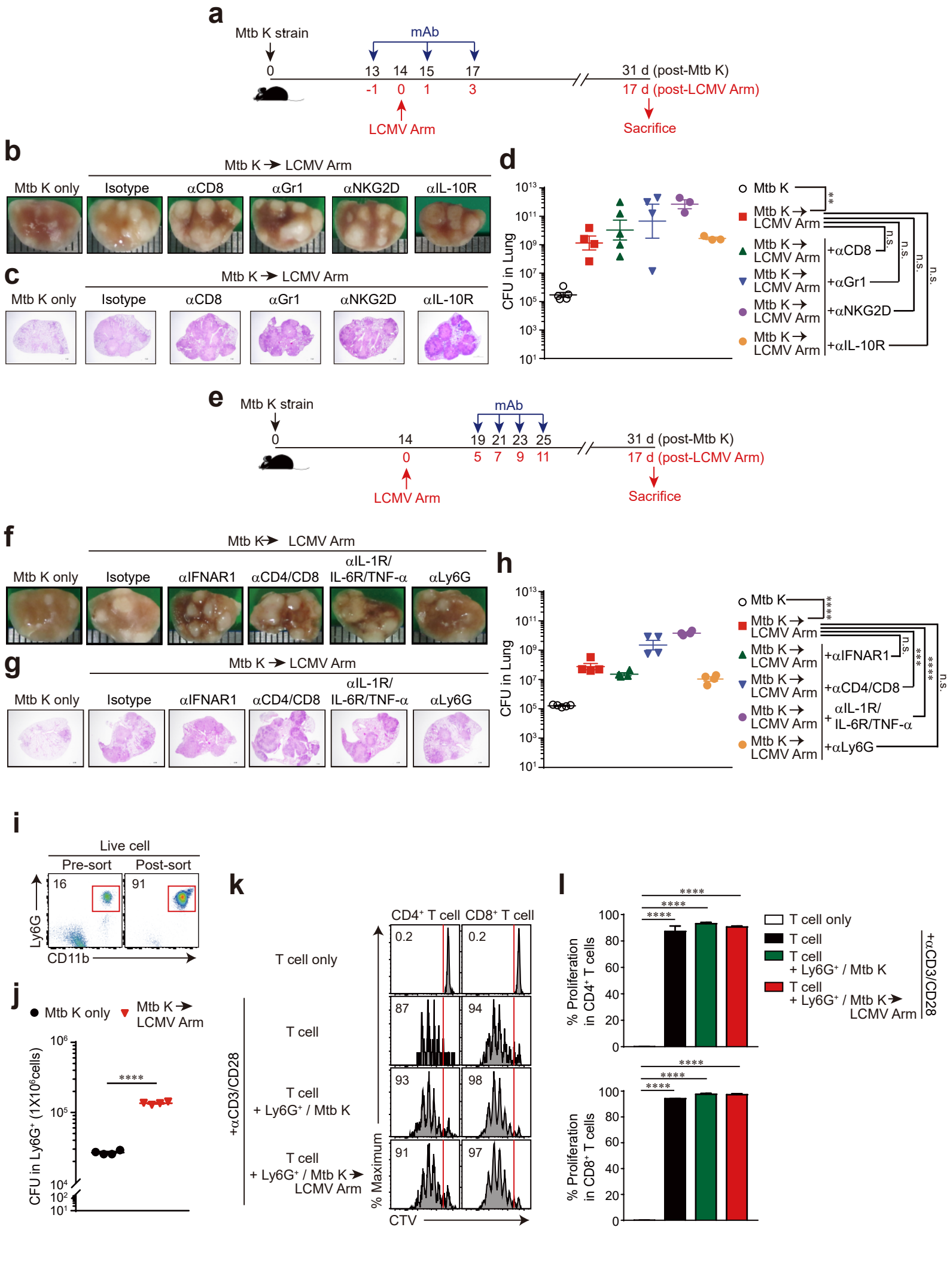

Supplementary Figure 5

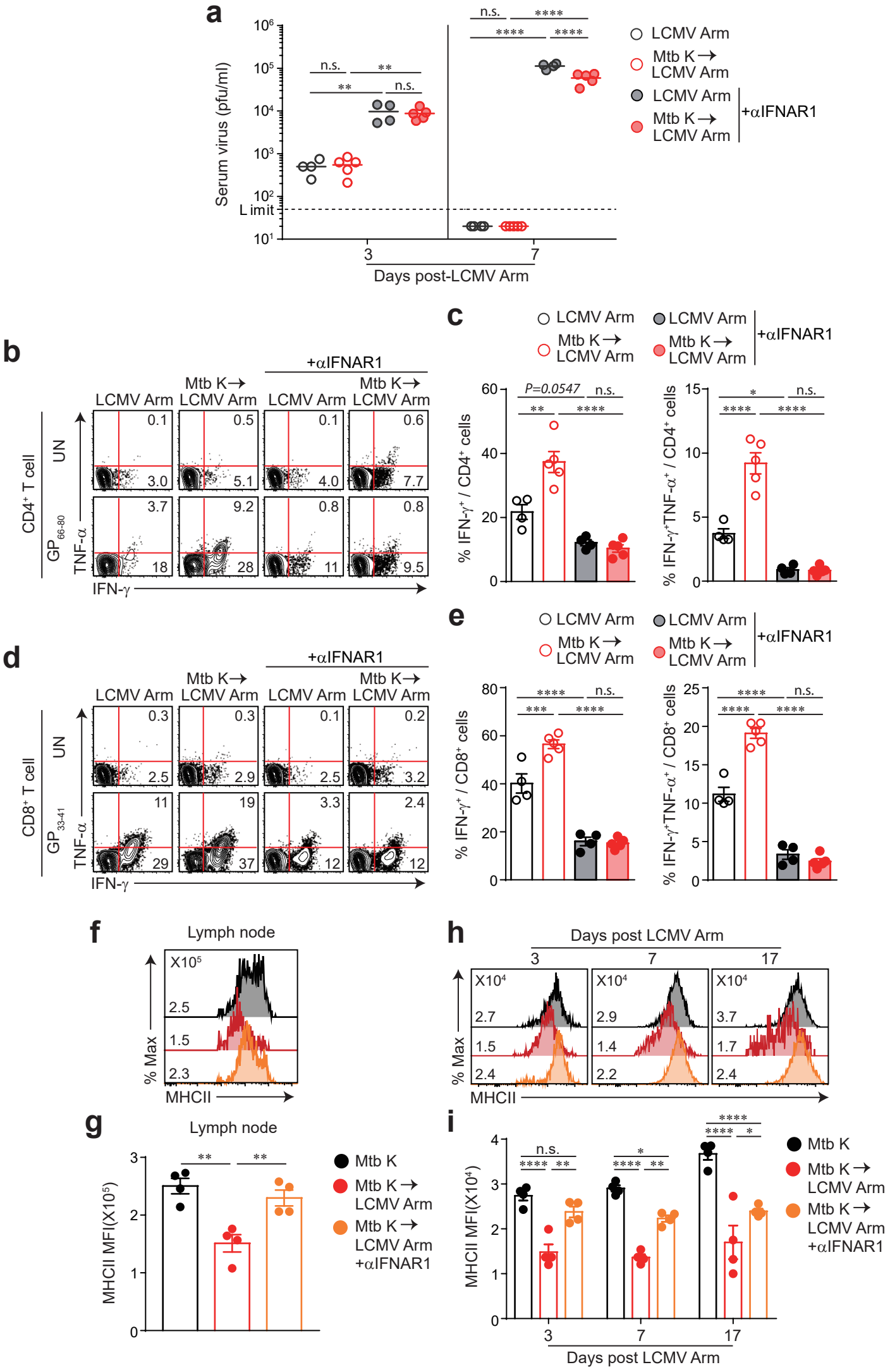

Supplementary Figure 6

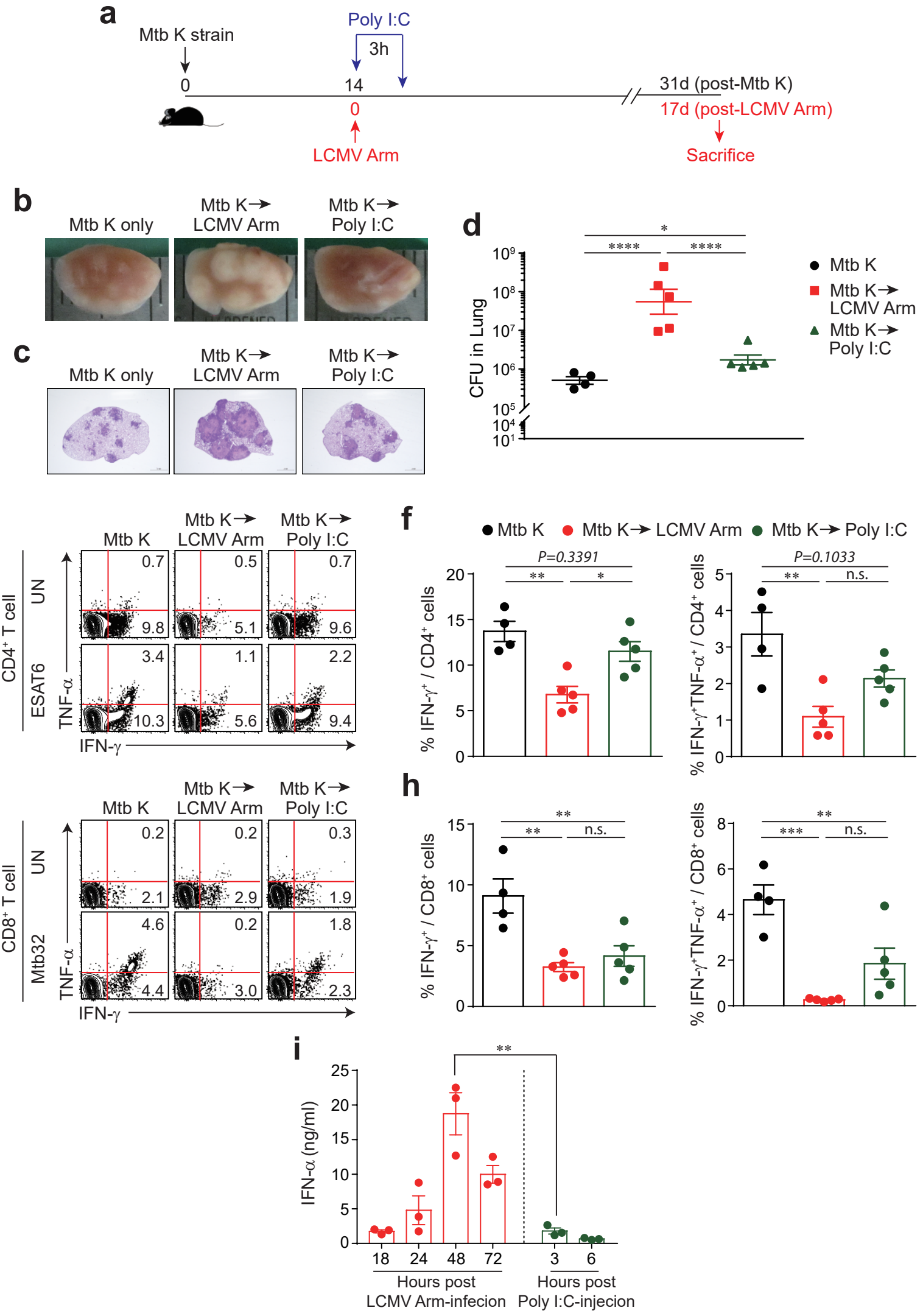

Supplementary Figure 7

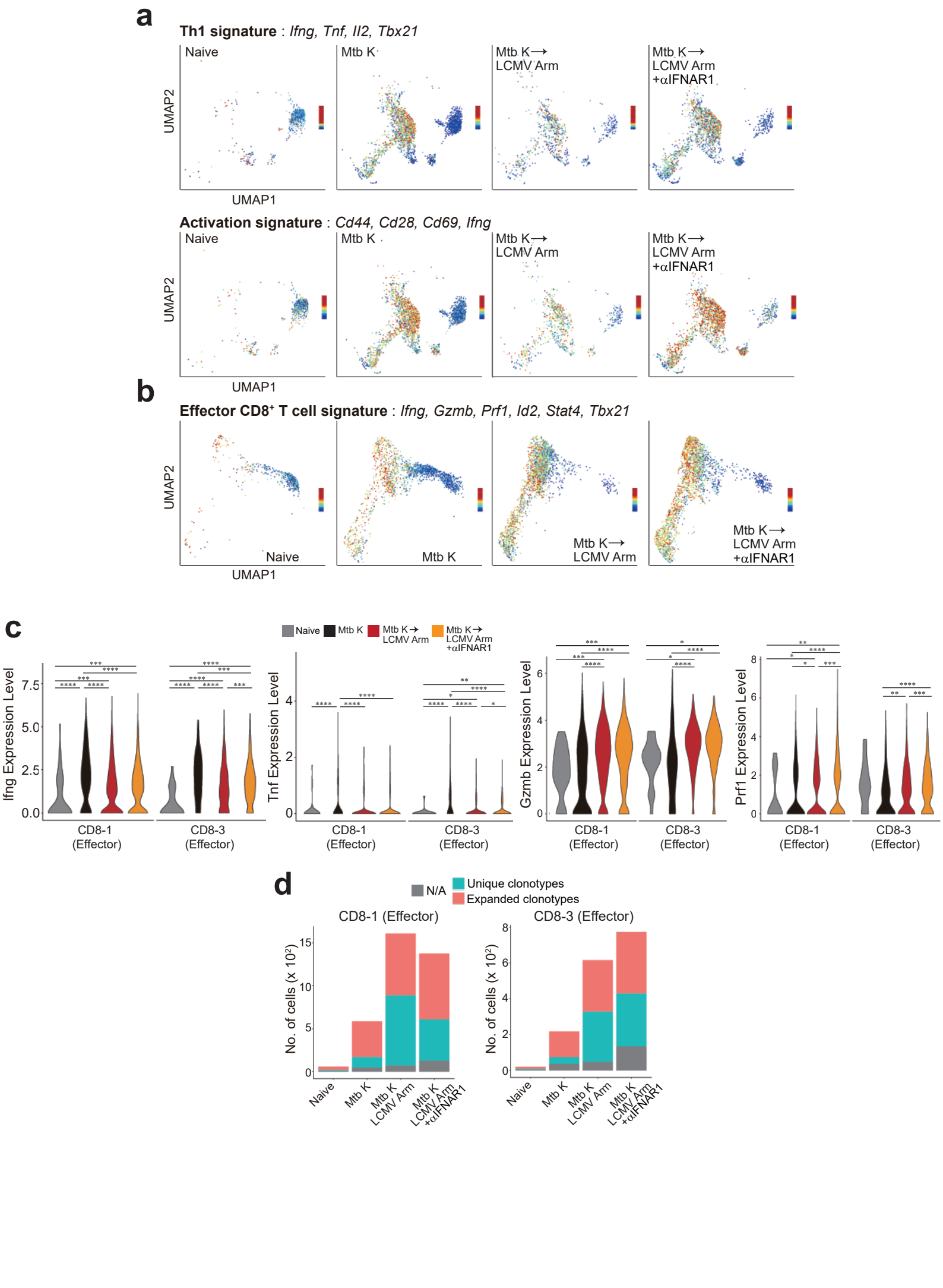

Supplementary Figure 8